We are IntechOpen, the world's leading publisher of Open Access books Built by scientists, for scientists

6,900
Open access books available

186,000
International authors and editors

200M
Downloads

Our authors are among the

154
Countries delivered to

TOP 1%
most cited scientists

12.2%
Contributors from top 500 universities

WEB OF SCIENCE™

Selection of our books indexed in the Book Citation Index in Web of Science™ Core Collection (BKCI)

Interested in publishing with us?
Contact book.department@intechopen.com

Numbers displayed above are based on latest data collected.
For more information visit www.intechopen.com

Chapter 5

Geometrical Draping of Nonwoven Fabrics

Abel Cherouat and Houman Borouchaki

Additional information is available at the end of the chapter

http://dx.doi.org/10.5772/61667

Abstract

This paper presents an optimization-based kinematic method for simulation of forming processes of nonwoven-fabric-reinforced composites using geometrical approach. The geometrical approach allows the defining of the 3D ply shapes, 2D flat pattern, and fiber distortions. Some numerical simulations of draping are proposed and compared with the experimental results.

Keywords: Woven and nonwoven, Carbon fabric, Draping, Geometrical approach, Fiber distortions

1. Introduction

Composite reinforced by woven or UD fabric is known to have high specific stiffness and, in combination with automatic manufacturing processes, makes it possible to fabricate complex components in various industry sectors (aircraft, boat, automotive, and military). Over the last years, the demand for high stiffness and strength and low-weight materials, such as fiber-reinforced plastics, has grown in the transport industry. Especially in the aeronautical industry, the use of woven-fabric-reinforced plastics has increased significantly. The main objective of aerospace industries is to reduce to half the amount of fuel by 2020 and at least 70% less by 2025. Composite manufacturing processes have undergone substantial evolution in recent years [1, 2]. Although the traditional layup process will remain the process of choice for some applications, new developments in Resin Transfer Molding (RTM), Liquid Composite Molding (LCM), or Sheet Molding Compound (SMC), low-temperature curing pre-pregs and low-pressure molding compounds have matured significantly, and are now being exploited in high-technology areas such as aerospace and automotive industries [3-7].

The manufacturing of reinforced composites needs different forming step in which the preform fabric (woven or nonwoven) takes the desired product's shape. The main deformation

INTECH
open science | open minds

© 2016 The Author(s). Licensee InTech. This chapter is distributed under the terms of the Creative Commons Attribution License (http://creativecommons.org/licenses/by/3.0), which permits unrestricted use, distribution, and reproduction in any medium, provided the original work is properly cited.

mechanism during forming of woven or nonwoven-reinforced composites is shear, which causes a change in fiber orientations. Fiber reorientation is one of the major factors causing fabric distortions, shrinking, and warpage defect. The fiber reorientation is an important factor that should be taken into account when designing composite products, since it will influence the overall thermomechanical properties and performance.

In this context, numerical simulation methods are needed to anticipate the performance of the final product, but also to predict the reinforcement preforming and the resin injection. Several modeling approaches have been developed in the literature to account for the evolution of the fiber orientation [8-11]. The earliest technique is based on discrete mapping approaches. In contrast to these mapping schemes, the constitutive behavior is required for continuum mechanical approaches [9, 12, 13].

The mapping approach, the so-called kinematic method, is used to determine the deformed shape of draped fabrics. The main assumptions are that the warp and weft fibers are inextensible, intersection points between warp and weft yarns are fixed during preforming, and the angle between warp and weft yarns are free. This method, where the fabric is placed progressively from an initial line, provides a close enough resemblance to hand-made draping [14-17].

The alternative to the kinematic approach consists of the use of Finite Element (FE) methods to simulate the fabric deformation under the boundary conditions prescribed by the forming process by considering the fabric as a homogeneous material using computationally efficient constitutive laws and continuum FEs. The limitation of the FE method is that the fabric is not really a continuum but can be more closely likened to a structure comprising discrete rods, possibly intertwined (for woven fabric), or loosely held together with stitching (for nonwoven fabric). The draping of composite fabric using a mechanical approach requires the resolution of equilibrium PDE's problems by the FE method. In general, in the case of complex surfaces, the boundary conditions are not well-defined and the contact between the surface and the fabric is difficult to manage [18, 19, 20]. Furthermore, the resolution of such a problem can be too long in CPU time and is detrimental to the optimization stage of draping regarding the initial fiber directions. All of these facts lead us to consider rather a kinematic approach, which is very fast and more robust, allowing simultaneously to define the stratification sequences and the flat pattern for different plies and to predict difficult impregnated areas that involve manual operation like dart insertion or, on the contrary, the shortage of fabric [21-38].

This paper presents an optimization-based method for simulation of forming processes of woven and nonwoven fabric reinforced composites using geometrical approach. Two draping simulation examples are given. These simulations are performed using the geometrical analysis computer code. For each example, we assume that a mesh of the mold to drape is given. The first example is the draping of woven fabric on double dome mold geometry. The second example shows the influence of the woven fabric and nonwoven on the draping process. The effects of the initial conditions (fiber orientation and start point) on the draped preform are discussed.

http://dx.doi.org/10.5772/61667

2. Kinematic approach

Several methods are used for predicting the fiber reorientation of the fabric. The geometrical model, also referred to as the kinematics or fishnet model is a widely used model to predict the resulting fiber reorientation for doubly curved fabric reinforced products [39, 40]. Based on a pinned-joint description of the weave, the model assumes inextensible fibers pinned together at their crossings, allowing free rotation at these joints. They analytically solved the fiber redistribution of a fabric orientated in the bias direction on the circumference of simple surfaces of revolution, such as cones, spheres, and spheroids. The resulting fiber orientations were solved as a function of the constant height coordinate of the circumference.

In the last 20 years, many authors have presented numerically based drape solutions, based on the same assumptions. The author refers to [6, 15, 41]. Typically, geometrical or kinematic fabric draping starts from a start point and two initial warp–weft fiber directions. Further points are then generated on the mold surface at a fixed equal distance from the previous points, creating a fabric mesh of quadrilateral element.

As the surface drape is generally complex and that the layup depends on the starting point and two ply directions, so there is no unique solution for the iterative geometrical simulation. This problem is generally solved by defining two fiber paths on the drape surface. Based on draping criteria such as maximum mold surface covering, minimum fabric drape covering, and minimum shear angle between warp and weft fibers, the geometrical approach can constitute the predimensioning or the preoptimization stage of the manufacturing in the product development process. The local change in composite properties must be taken into account to predict the properties of a composite product.

In this study, we propose a new discrete geometrical algorithm that takes into account the true geometry of the nonwoven fabric mesh element plotted onto the surface. The proposed approach is based on the fishnet method for which a fabric mesh element is subjected only to shear deformation. The difficulty of such a method is the mapping of the nonwoven fabric mesh element onto any surface [42].

Such a fabric mesh element is then defined by a curved quadrilateral, whose edges are geodesic lines with the same length plotted onto the surface to drape. Given three vertices of the fabric mesh element on the surface, we propose an optimization algorithm to define the fourth vertex of the fabric mesh element. The nonwoven fabric is a fabric-like material made from long fibers and expandable filaments bonded together by mechanical weaving, in order to obtain suitable shear deformation. If the shear angles of fibres are significant, then is allowed step-by-step elongations of filaments and this through an optimized iterative procedure.

Let Σ denote the surface of the part to drape and we assume that a geometrical mesh $\mathbf{T}_{\boldsymbol{\Sigma}}$ of surface is known. Let $\mathcal{F}$ be the woven composite fabric modeled by two families (warp and weft) of mutually orthogonal and inextensible fiber described by the local coordinates $x=(\xi, \eta)$. These families constitute regular quadrilateral fabric mesh $\mathbf{T}_{\mathbf{F}}$ of the fabric $\mathcal{F}$ (Fig. 1 gives example of draping steps of complex surface). The problem of geometrical draping of $\mathcal{F}$ onto the surface Σ consists of calculating each node displacement of fabric mesh $\mathbf{T}_{\mathbf{F}}$ with a point of the surface mesh $\mathbf{T}_{\boldsymbol{\Sigma}}$ such that the lengths of the edge of the corresponding mesh $\mathbf{T}_{\mathbf{F}}^{\boldsymbol{\Sigma}}$ on the

surface are preserved (no extensible). This problem presents infinity of solutions depending on:

1. Starting point P associated with a node of fabric $\mathbf{T}_{\mathbf{F}}^{\Sigma}$
2. Initial warp-and-weft orientation θ

Thus, to ensure a unique solution, we suppose that the points of impact on the part surface as well as the fabric orientation are given. The draping scheme is given by the following step [31]:

1. Choose a starting point A (corresponding to the point of impact of the machine: to drape) on the surface on geometrical part mesh $\mathbf{x}_0^{\Sigma}=(\xi_0, \eta_0)$.
2. Compute iteratively the warp nodes of $\mathbf{T}_{\mathbf{F}}^{\Sigma}$, classified as $\alpha-$**nodes**, from the starting point, associated with nodes (ξ, η_0) of $\mathbf{T}_{\mathbf{F}}$.
3. Compute iteratively step-by-step the weft nodes of $\mathbf{T}_{\mathbf{F}}^{\Sigma}$, classified also as $\alpha-$**nodes**, from the starting point, associated with nodes (ξ_0, η) of $\mathbf{T}_{\mathbf{F}}$.
4. Compute iteratively cell-by-cell all the other nodes of $\mathbf{T}_{\mathbf{F}}^{\Sigma}$, classified as $\beta-$**nodes**, from x_0 and the nodes associated with nodes (ξ, η_0) and (ξ_0, η) of $\mathbf{T}_{\mathbf{F}}$.

The nodes of $\mathbf{T}_{\mathbf{F}}^{\mathbf{S}}$ associated with nodes (ξ, η_0) and (ξ_0, η) of $\mathbf{T}_{\mathbf{F}}$ and the $\alpha-$**nodes** are located on the surface along the geodesic lines emanating from the point of impact. Regarding the $\beta-$**nodes**, various algorithms are proposed. Most of them use an analytical expression of the surface and formulate the draping problem in terms of nonlinear partial differential equations. Other algorithms are also proposed to simplify these equations by using a finite element discretization of the surface by flat triangular face (i.e., a mesh of the surface). Based on this latter approach, we propose a new algorithm. $\beta-$**nodes** are computed by solving an optimization problem corresponding to determine a vertex of an equilateral quadrilateral plotted on the surface from the data of the three other vertices. This optimization problem concerns the following:

1. **Problem 1**: Determine the geodesic curve with a given length from a point of surface according to a given woven or nonwoven fabric direction. This problem is solved by isometrically unfolding the mesh elements along a given direction. The geodesic curve is then a strait segment. The latter is then mapped back to the surface using the unfolded elements to obtain the desired geodesic line.
2. **Problem 2**: Determine the directions of two geodesic curves with a given length from two different points of surface reaching to the same point. To solve the second problem, an iterative approach is applied to find the searched directions. Let us consider a starting point P; its successor P_1 along a warp direction and its successor P_2 along a weft direction (see Fig. 1).

The problem is to find point Q such that curve P_1Q and curve P_2Q are the geodesic lines with a given length. Thus, we have to determine the directions $\vec{u}_1$ and $\vec{u}_2$ of these geodesic lines from

http://dx.doi.org/10.5772/61667

P_1 and P_2. Initially, these directions are set to $\vec{u}_1=\overrightarrow{PP_2}$ and $\vec{u}_2=\overrightarrow{PP_1}$ and geodesic curves P_1Q_1 and P_2Q_2 are obtained. Then iteratively these directions are set to $\vec{u}_1=\overrightarrow{P_1Q_{12}}$ and $\vec{u}_2=\overrightarrow{P_2Q_{12}}$, where $Q_{12}=(P_1+P_2)/2$; while Q_1 is different than Q_2.

The proposed algorithm can easily extended to the case of nonwoven intended, if the shear angle at the point Q is greater than a threshold value depending on nonwoven properties. In order to obtain suitable deformation of nonwoven during the draping operation, the algorithm to find the optimized position of the point Q is based on the shear angle criterion. If the shear angles are lower than the locking angle, the algorithm is identical to the case of woven fabric, and if the shear angles are significant, then the algorithm allows step-by-step elongations of filaments and this through an optimized iterative procedure.

The kinematic approach is well-adapted to preliminary design level. It is based on a modified MOSAIC algorithm, which is suitable to generate a regular quad mesh representing the layup of the curved surfaces. The method is implemented in the GeomDrap software, which is now integrated in the ESI-Pam QUICK software. Pam QUICK software allows to estimate a fiber quality charter (showing distortion of fiber, drop rate, and drape surface ratio) to predict local bending due to overlapping of the fibers in the shear exceeds the limit value depending on the properties of the fabric. It can be used to optimize the draping process by improving the layup directions or the marker data location [43].

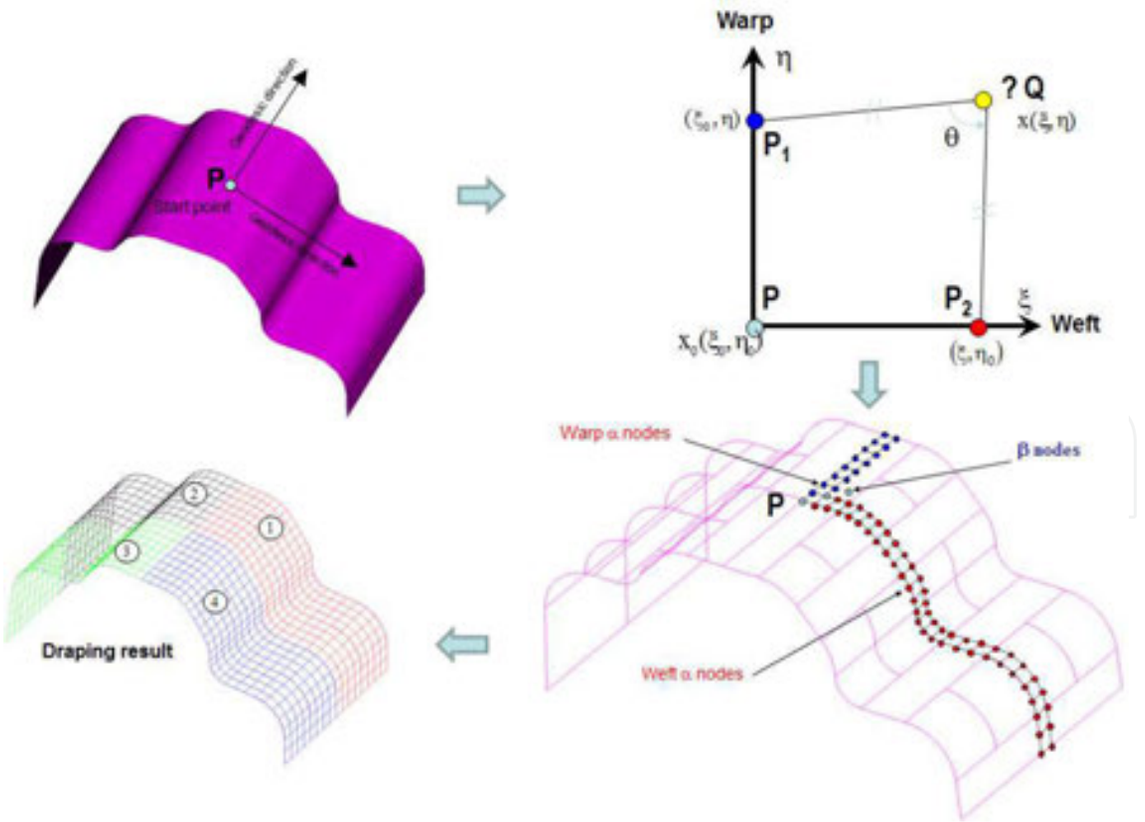

Figure 1. *Geometrical draping steps of woven composite fabric*

Figure 1. Geometrical draping steps of woven composite fabric

3. Applications

The simulated results for the complex geometry are presented here. Draping is simulated with a geometrical draping method described in section 2. For each example, we assume that a mesh of the mold to drape is given. The material properties of the composite product can be predicted from the local fiber volume fraction and the shear angle, which represents the angle between the local warps/weft fiber directions. In the first example, we present the draping of woven or nonwoven composite mold on non-

quadrilateral shells elements. In order to assess the influence of the initial constraints, two fabric orientations are considered. The initial contact point P of the drape is the center point of the hemisphere part of the mold and two fiber directions, 0° and 45° fabric orientations are presented.

In order to compare the experimental warp/weft angles with the predicted results, two cross sections along the symmetrical line noted L1 (for 45° ply orientation) and the diagonal line noted L2 (for 0° ply orientation) where most shearing occurs are examined (see Fig. 2).

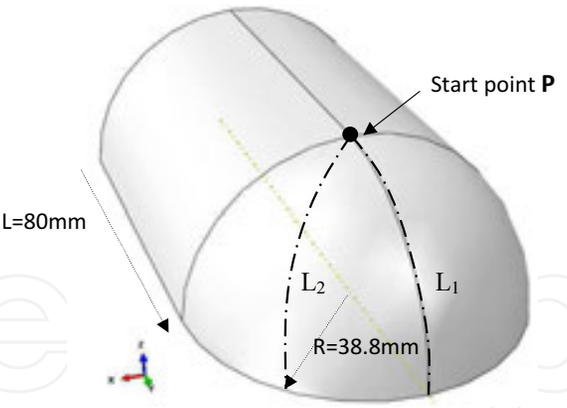

Figure 2. *Schematic view of the half hemisphere connected by a half cylinder*

Figure 2. Schematic view of the half hemisphere connected by a half cylinder

3. Applications

The simulated results for the complex geometry are presented here. Draping is simulated with a geometrical draping method described in section 2. For each example, we assume that a mesh of the mold to drape is given. The material properties of the composite product can be predicted from the local fiber volume fraction and the shear angle, which represents the angle between the local warp/weft fiber directions. In the first example, we present the draping of woven or nonwoven composite mold on non developable geometry in order to validate the proposed model. In this case, we compare the fiber distribution and distribution of the shear angle between the fibers in the deformed fabric. In this example, it is necessary to take the effect of the excessive fiber distortion and the cutting chisel on the draping process of half hemisphere connected by a half cylinder. Comparison with experimental results is illustrated in order to validate the proposed approach. The second example compares the draping of woven and nonwoven carbon fabric on complex mold. The third and the last example show the influence of the initial start point and fiber orientation on the flat pattern of the nonwoven fabric.

3.1. Validation of the geometrical algorithm

The highest procedure presented above is used to simulate the draping of composite woven dry fabric on complex mold. In this case, we consider the draping of woven carbon fabric on two half hemispheres with a radius of R = 38.8 mm connected by a half cylinder with a length of L = 80 mm (see Fig. 2). Drape experiments results have been performed by [43]. Boundary conditions consist of an initial start point and warp/weft directions in this point. The mold surface is modeled using triangular and quadrilateral shells elements. In order to assess the influence of the initial constraints, two fabric orientations are considered. The initial contact point P of the drape is the center point of the hemisphere part of the mold and two fiber directions, 0° and 45° fabric orientations are presented.

In order to compare the experimental warp/weft angles with the predicted results, two cross sections along the symmetrical line noted L1 (for 45° ply orientation) and the diagonal line noted L2 (for 0° ply orientation) where most shearing occurs are examined (see Fig. 2).

In order to evaluate qualitatively the drape simulation, the enclosed fiber angle was measured in the area between the half hemisphere and cylinder at the longitudinal and diagonal axis of the mold. Figure 3 shows the resulting 3D surface draping for [0°/90°] and [-45°/+45°] fiber orientations. One can notice that in both cases, the mold is completely draped but the shear angles between warp and weft fibers are very excessive (greater than 80°) which is impossible and can induce defects in the composite properties after resin injection or polymerization. Figure 4 presents shaded contours interpolated from the map of the shear angles for [0°/90°] ply orientation and Fig. 5 presents shear angles for [-45°/+45°] ply orientation. The shear angle for both [0°/90°] and [-45°/+45°] draping is large (70°) but the maximum shear angle localization is different. The evolution of a draping simulation shows that the red areas indicate that with this fabric, a single sheet will not be able to cover the hemisphere without creasing. Splits can be added to the fabric, or fiber stretching can be allowed in order to minimize the shear angle.

In order to optimize the draping operation and drape completely the mold without excessive fiber distortion (fiber locking [10]) depending on fabric properties, it is necessary to:

- Make cuts chisel along the line C_2 for [0°/90°] fiber orientation (Fig. 4a) and along the line C_1 for [-45°/+45°] fiber orientation (Fig. 4b). With the cutting chisel operation, the shear limit reached 38° in the case of [0°/90°] and 68° in the case of [-45°/+45°].
- Allow warp and weft fiber stretching of 20%. Without the cutting chisel operation, the mold is completely draped and the shear limitreached 52° in the case of [0°/90°] fiber orientation (Fig. 5a) and 89° in the case of [-45°/+45°] (Fig. 5b).

To compare the predicted shear angles with the experimental result given by [44], measurements of angles along the lines where the highest shear angles occur were performed. From Fig. 6 it can be

http://dx.doi.org/10.5772/61667

In order to evaluate qualitatively the drape simulation, the enclosed fiber angle was measured in the area between the half hemisphere and cylinder at the longitudinal and diagonal axis of the mold. Figure 3 shows the resulting 3D surface draping for [0°/90°] and [-45°/+45°] fiber orientations. One can notice that in both cases, the mold is completely draped but the shear angles between warp and weft fibers are very excessive (greater than 80°) which is impossible and can induce defects in the composite properties after resin injection or polymerization. Figure 4 presents shaded contours interpolated from the map of the shear angles for [0°/90°] ply orientation and Fig. 5 presents shear angles for [-45°/+45°] ply orientation. The shear angle for both [0°/90°] and [-45°/+45°] draping is large (70°) but the maximum shear angle localization is different. The evolution of a draping simulation shows that the red areas indicate that with this fabric, a single sheet will not be able to cover the hemisphere without creasing. Splits can be added to the fabric, or fiber stretching can be allowed in order to minimize the shear angle.

In order to optimize the draping operation and drape completely the mold without excessive fiber distortion (fiber locking <50°) depending on fabric properties, it is necessary to either:

- Make cuts (chisel along the line C) for [0°/90°] fiber orientation (Fig. 4a) and along the line C1 for [-45°/+45°] fiber orientation (Fig. 4b). With the cutting chisel operation, the shear limit reached 38° in the case of [0°/90°] and 68° in the case of [-45°/+45°].
- Allow warp and weft fiber stretching of 20%. Without the cutting chisel operation, the mold is completely draped and that shear limit reached 52° in the case of [0°/90°] fiber orientation (Fig. 5a) and 89° in the case of [-45°/+45°] (Fig. 5b).

concluded that for the [0°/90°] ply orientation along the diagonal line L2, the agreement between the experimental shear angles and the predicted draping results is good. On the other side, for [-45°/+45°] ply orientation along the symmetrical line L1, the predicted results do not agree at all with the experimental values. The oversimplification of the fabric deformation in the geometrical model gives shear angles up to 89° in case of the 45° ply orientation, which is impossible for woven fabric. The geometrical model is used with a cutoff shear angle based either on an experimentally determined locking angle, or the maximum orientation that the designer is prepared to tolerate. When defining a cutoff angle of 38°, which equals the experimentally determined locking angle, one can, in this case, drape the mould which has high shear angles with nonwoven fabric.

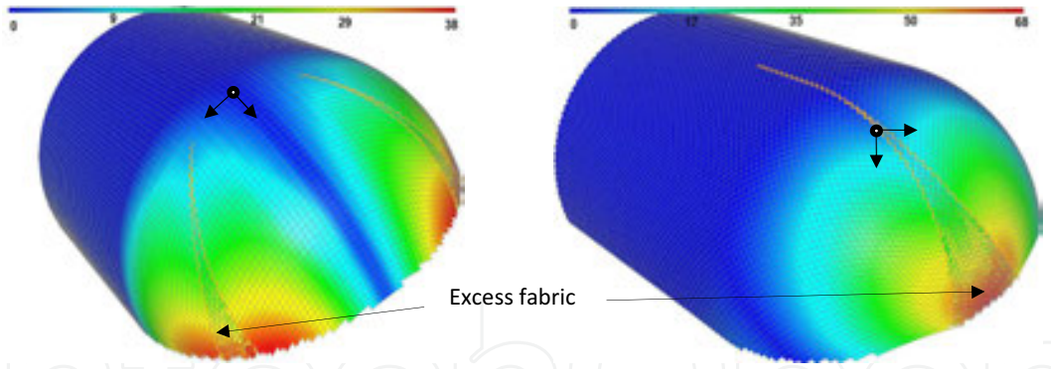

(a) [0°/90°] ply orientation *(b) [-45°/+45°] ply orientation*

Figure 3. *Drape results on shear angles of 0° and 45° ply orientations*

Figure 3. Drape results on shear angles of 0° and 45° ply orientations

To compare the predicted shear angles with the experimental result given by [44], measurements of angles along the lines where the highest shear angles occur were performed. From Fig. 6 it can be concluded that for the [0°/90°] ply orientation along the diagonal line L2, the agreement between the experimental shear angles and the predicted draping results is good. On the other side, for [-45°/+45°] ply orientation along the symmetrical line L1, the predicted results do not agree at all with the experimental values. The oversimplification of the fabric deformation in the geometrical model gives shear angles up to 89° in case of the 45° ply orientation, which is impossible for woven fabric. The geometrical model is used with a cutoff

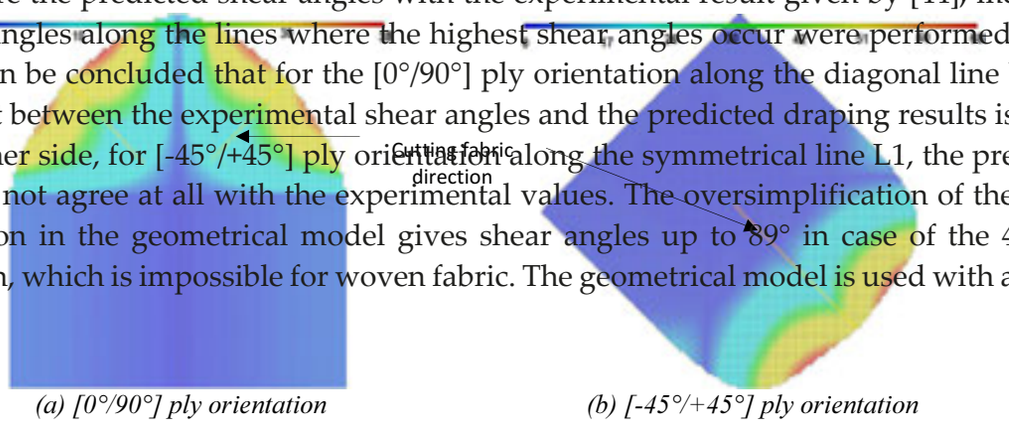

(a) [0°/90°] ply orientation *(b) [-45°/+45°] ply orientation*

Figure 4. *2D flat pattern results of 0° and 45° ply orientations*

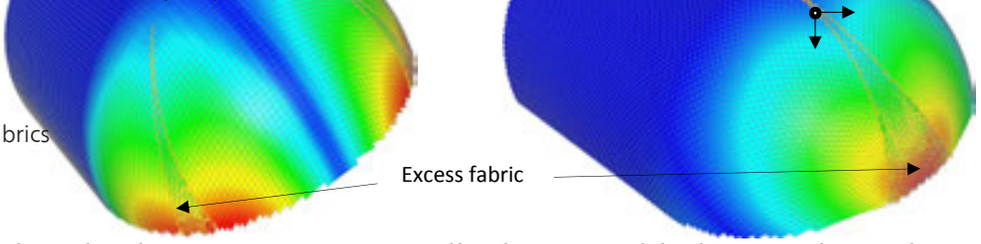

(a) [0°/90°] ply orientation *(b) [-45°/+45°] ply orientation*

Figure 3. *Draape results on shear angles of 0° and 45° ply orientations*

shear angle based either on an experimentally determined locking angle, or the maximum orientation that the designer is prepared to tolerate. When defining cutoff angle of 38°, which equals the experimentally determined locking angle, one can, in this case, drape the mould, which has high shear angles, with nonwoven fabric.

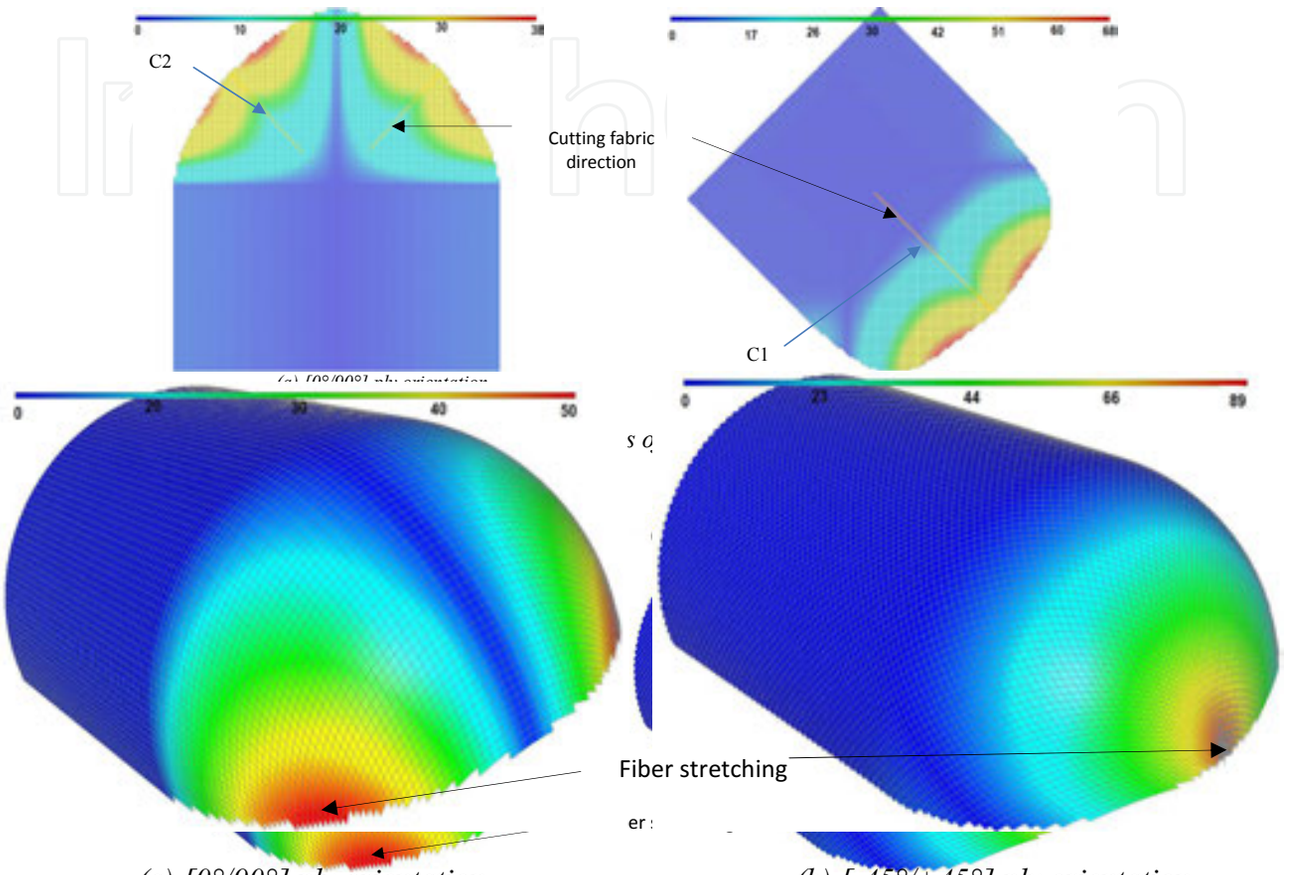

(a) [0°/90°] ply orientation *(b) [-45°/+45°] ply orientation*

(a) [0°/90°] ply orientation *(b) [-45°/+45°] ply orientation*

Figure 5. *Optimized drape results on shear angles of 0° and 45° ply orientations*

Figure 5. *Optimized drape results on shear angles of 0° and 45° ply orientations*

Figure 5. Optimized drape results on shear angles of 0° and 45° ply orientations

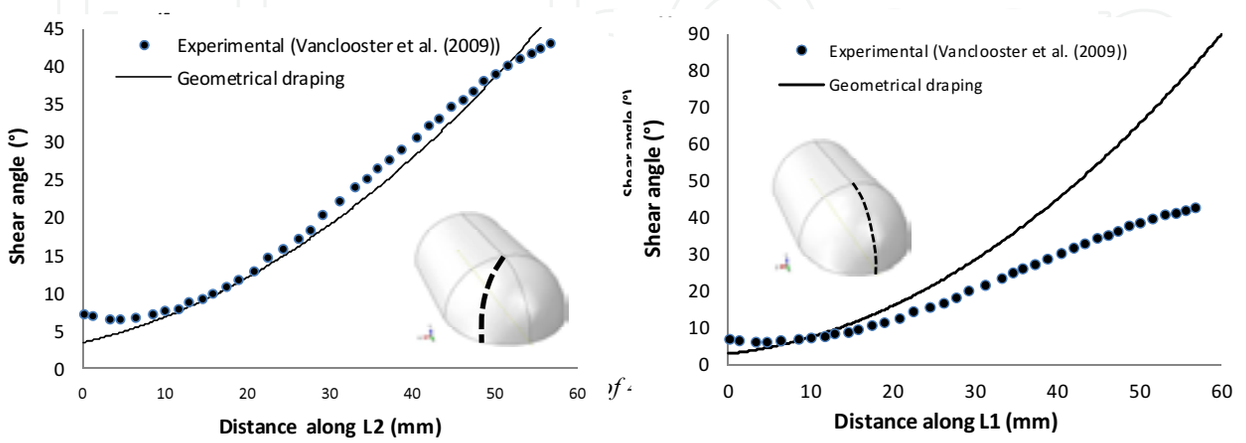

Figure 6. *Shear angle along (a) the line L2 of 45° orientation and (b) along L2 of 0° orientation*

3.2. Comparison of woven and nonwoven fabric draping

The second example concerns the draping of woven and nonwoven carbon fabric on complex plastic mold. The initial rectangular taffeta fabric dimensions are: length = 700 mm and width = 350 mm (Fig. 7). The start point P in the simulation was the center of mass and the initial fiber direction is 45° with the geodesic mold directions (see Fig. 8). Figure 9 shows the resulting 3D draping for the woven and

http://dx.doi.org/10.5772/61667

3.2. Comparison of woven and nonwoven fabric draping

The second example concerns the draping of woven and nonwoven carbon fabric on complex plastic mold. The initial rectangular taffeta fabric dimensions are: length = 700 mm and width = 350 mm (Fig. 7). The start point P in the simulation was the center of mass and the initial fiber direction is 45° with the geodesic mold directions (see Fig. 8). Figure 9 shows the resulting 3D draping for the woven and nonwoven fabric. We can note that all part surfaces are completely draped with woven and nonwoven fabric but with defect, the outline shapes of flat pattern are different, and the location of the maximum shear angles is the same as in the draped surface. Figure 10 presents shaded contours interpolated from the map of the fiber shear angles. For the draping of the surface with nonwoven fabric, we note that also all part of surface is completely draped with large shear angle (θ>85°) with fiber disentanglement and junction unraveling. For drape orientation, the results from geometrical model agree with the experimental results. One can conclude, in the considered cases, the draped surface of the product with 45° fiber orientation with woven or nonwoven fabric is impossible without cutting chisel operation. The very excessive shear angles induce defects and superposition of the cross-ply in the composite part after resin injection or polymerization.

very excessive shear angles induce defects and superposition of the cross-ply in the composite part after resin injection or polymerization.

very excessive shear angles induce defects and superposition of the cross-ply in the composite part after resin injection or polymerization.

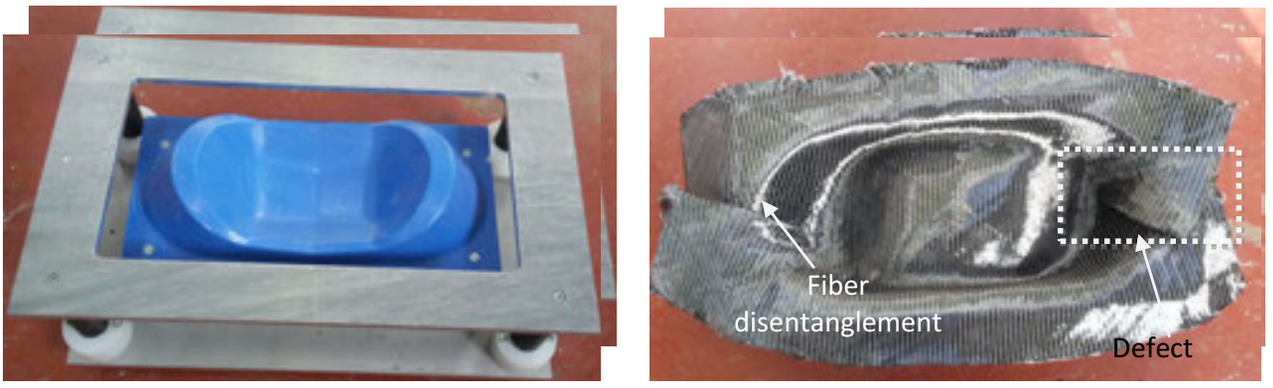

Figure 7. Mold design and experimental nonwoven draping result

Figure 7. *Mold design and experimental nonwoven draping result*

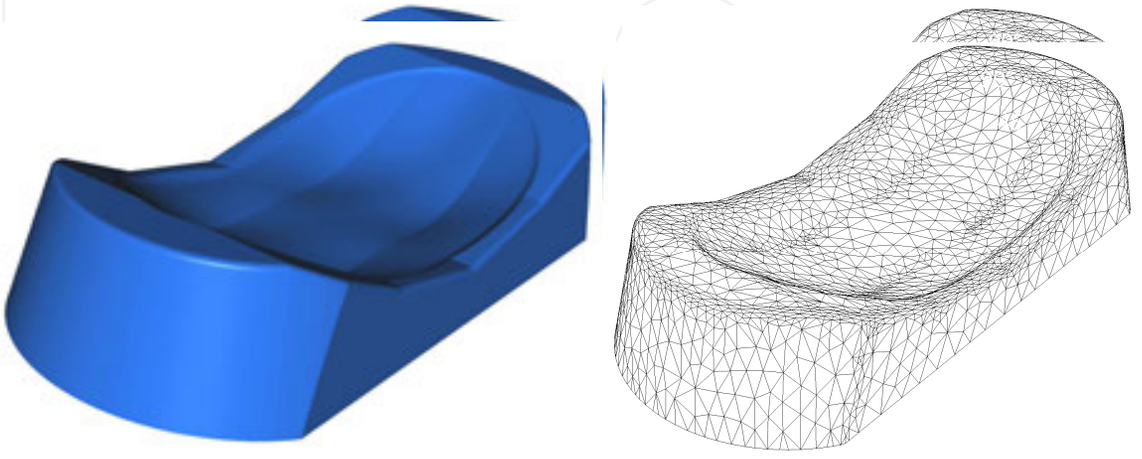

Figure 8. CAD and mesh of the mold

Figure 8. *CAD and mesh of the mold*

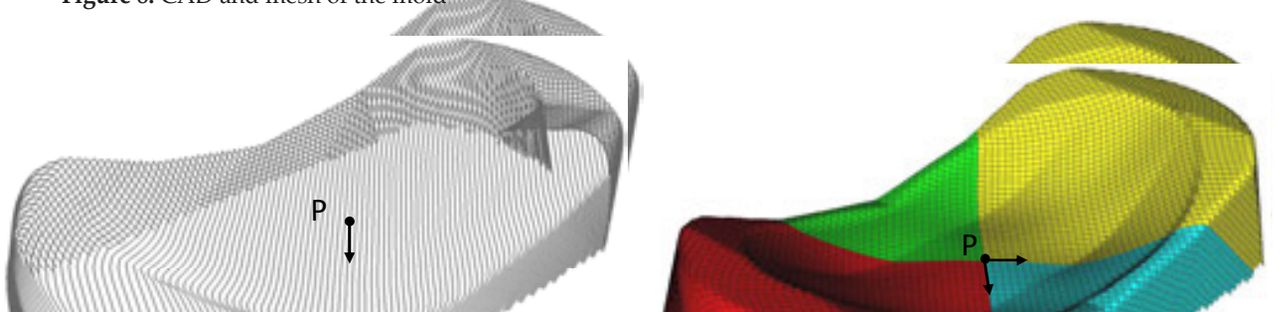

Figure 8. *CAD and mesh of the mold*

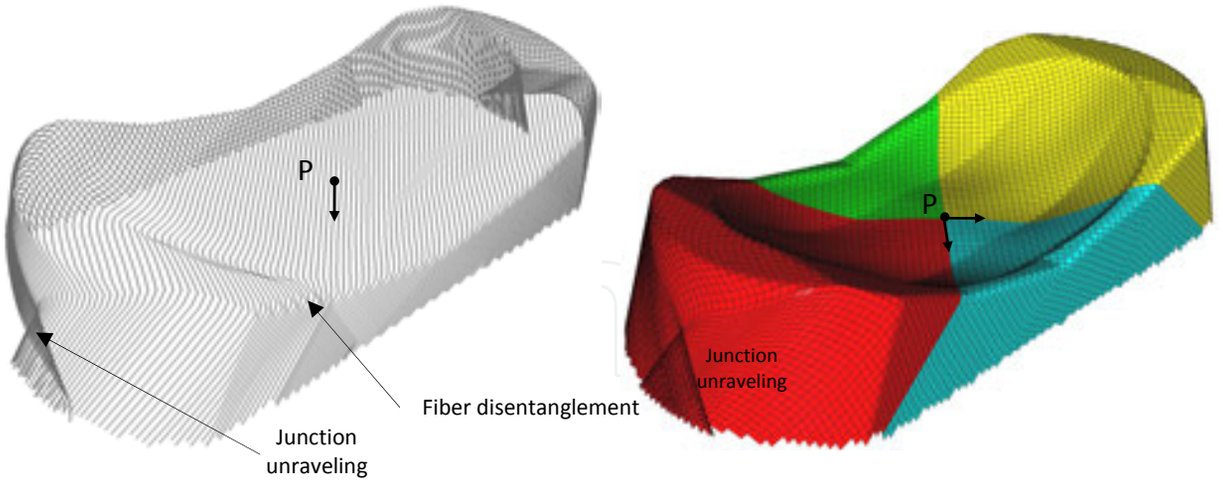

(a) Nonwoven fabric *(b) Woven fabric*

Figure 9. *3D geometrical draping using UD fabric and woven carbon fabric*

Figure 9. 3D geometrical draping using UD fabric and woven carbon fabric

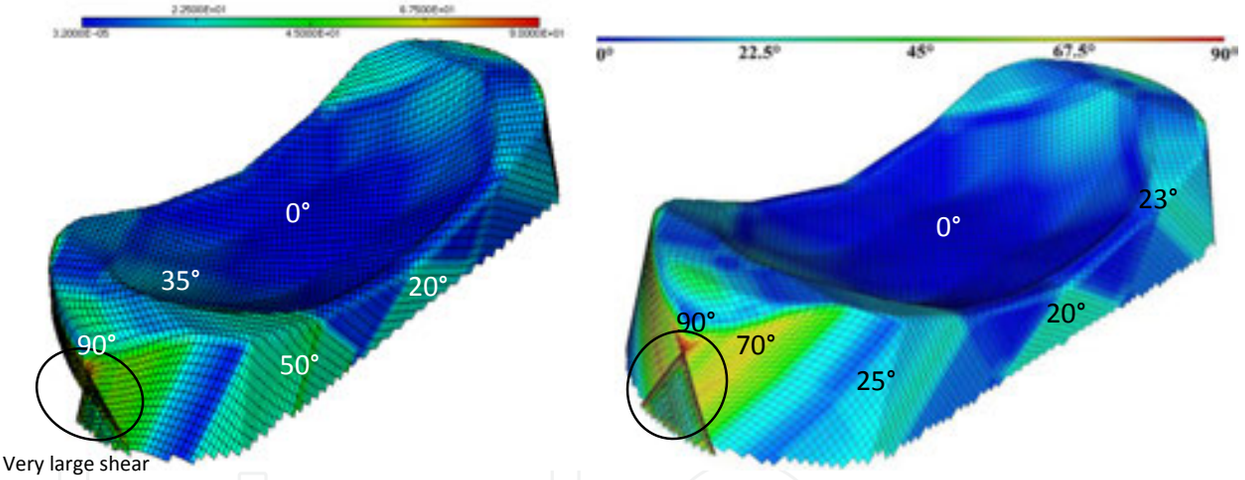

9

Figure 10. *Shear angle of draped UD fabric and woven carbon fabric*

Figure 10. Shear angle of draped UD fabric and woven carbon fabric

3.3. Effect of nonwoven fabric orientation

3.3. Effect of nonwoven fabric orientation

The mechanical response of nonwoven fabrics exhibits an anisotropic response biased toward the direction of preferential alignment of constituent fibers. The deformation mechanisms governing the fabric response under bias-loads include textural evolution by means of reorientation of constituent fibers, fiberstretch, relative fiber slip, as well as fiber disentanglement and junction unraveling.

The mechanical response of nonwoven fabrics exhibits an anisotropic response biased toward the direction of preferential alignment of constituent fibers. The deformation mechanisms governing the fabric response under bias-loads include textural evolution by means of reorientation of constituent fibers, fiberstretch, relative fiber slip, as well as fiber disentanglement and junction unraveling.

The proposed mold shape is now draped geometrically using three fiber orientations. Here, only the predicted fiber orientations on the mold shape are compared. Figures 11, 12, and 13 show the resulting 3D nonwoven fabric draping for the 0°, 90°, and 45° drape orientations, respectively, and the corresponding shaded contours interpolated from the map of the fiber orientation. From these figures it can be concluded that for the same initial contact point, the shear angle ($\theta > 80°$) localization is different and level is highly dependent on the mold geometry and the boundary conditions. Various defects such as unraveling of weaving and disentanglement of the fibers produced during the layup and may have effects on the quality of the final composite part after the injection of resin or polymerization.

The proposed mold shape is now draped geometrically using three fiber orientations. Here, only the predicted fiber orientations on the mold shape are compared. Figures 11, 12, and 13

http://dx.doi.org/10.5772/61667

The mechanical response of nonwoven fabrics exhibits an anisotropic response biased toward the direction of preferential alignment of constituent fibers. The deformation mechanisms governing the fabric response under bias-loads include textural evolution by means of reorientation of constituent fibers, fiber stretch, relative fiber slip, as well as fiber disentanglement and junction unraveling.

The proposed mold shape is now draped geometrically using three fiber orientations. Here, only the predicted fiber orientation on the mold shape are compared. Figs. 10, 11, 12 and 13 show the resulting 3D nonwoven fabric draping for the 0°, 90°, and 45° drape orientations, respectively, and the corresponding shaded contours interpolated from the map of the fiber orientation. From these figures it can be concluded that for the same initial contact point, the shear angle ($\theta > 80°$) localization is different and level is highly dependent on the mold geometry and the boundary conditions. Various defects such as unraveling of weaving and disentanglement of the fibers produced during the layup and may have effects on the quality of the final composite part after the injection of resin or polymerization.

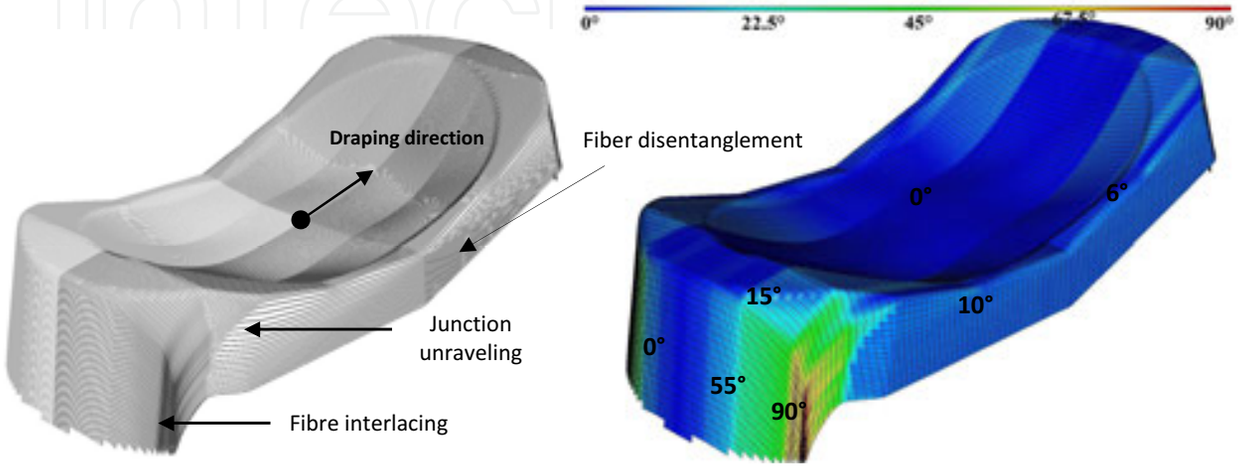

Figure 11. *3D draping and iso-values of fiber angles of the 0° nonwoven draping*

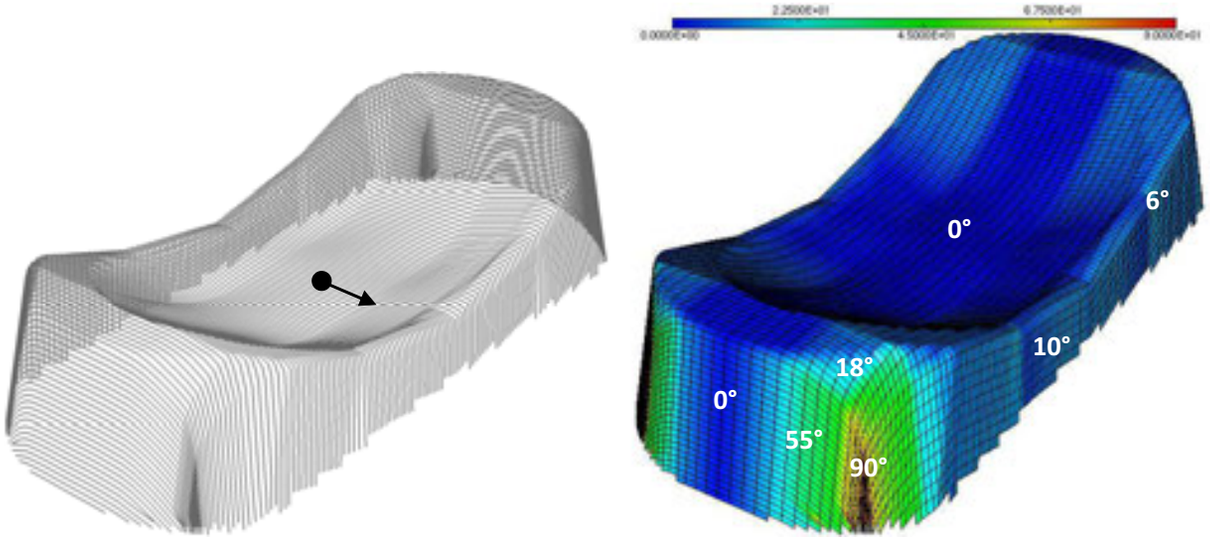

Figure 12. *3D draping and iso-values of fiber angles of the 90° nonwoven draping*

3.4. Effect of the draping start point

To study the effect of the initial start point on the draping results, a surface double dome is draped by non-woven fabric (Fig. 14). The mold shape consists of two coinciding hemispheres with different radii (small sphere radius R = 75 mm and large sphere raditis R = 100 mm). The

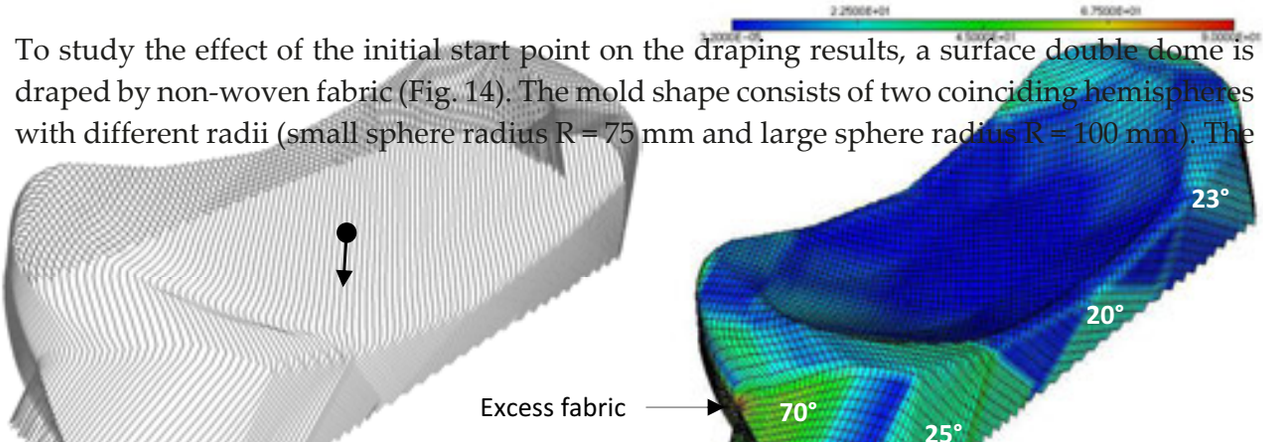

Figure 12. *3D draping and iso-values of fiber angles of the 90° nonwoven draping*

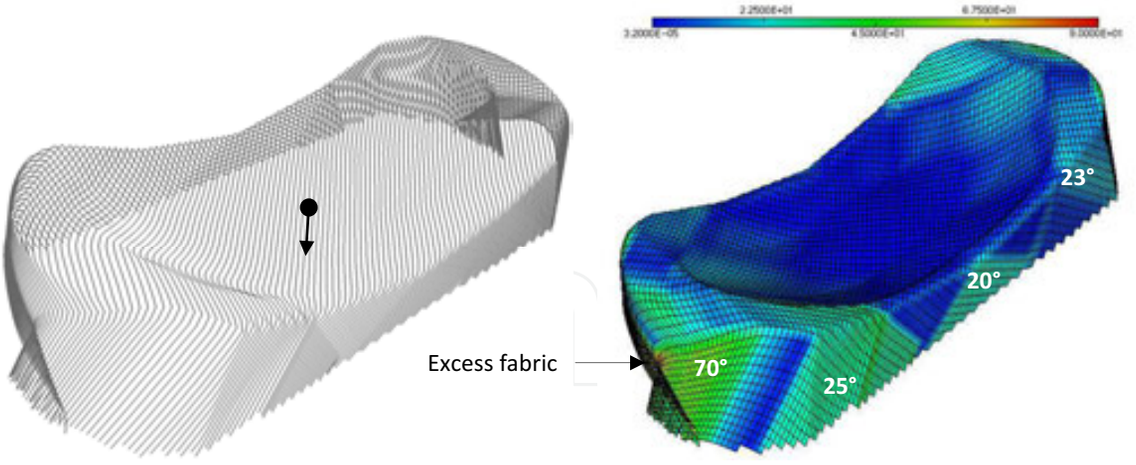

Figure 13. 3D draping and iso-values of fiber angles of the 45° nonwoven draping.

Figure 13. *3D draping and iso-values of fiber angles of the 45° nonwoven draping*

initial start point P in the simulation was chosen as the top of the small (D1) or the large hemisphere part (D2). The initial ply orientation was perpendicular to the main axis of the mold (Fig. 15). Here, the predicted 3D draping, shear fiber orientations on the double dome shape, and the 2D flat pattern are compared [45].

3.4. Effect of the draping start point

To study the effect of the initial start point on the draping results, a surface double dome is draped by non-woven fabric (Fig. 14). The mold shape consists of two coinciding hemispheres with different radii (small sphere radius R = 75 mm and large sphere radius R = 100 mm). The initial start point P in the simulation was chosen as the top of the small (D1) or the large hemisphere part (D2). The initial ply orientation was perpendicular to the main axis of the mold (Fig. 15). Here, the predicted 3D draping, shear fiber orientations on the double dome shape, and the 2D flat pattern are compared [45].

1. At first glance, the results look very similar for the draping on the smaller sphere start point and on the large sphere start point (see Figs. 16 and 17). Both cases predict the same fiber directions along the main mold perpendicular axis and the same 2D fabric flat pattern (Fig. 19).

1. At first glance, the results look very similar for the draping on the smaller sphere start point and on the large sphere start point (see Figs. 16 and 17). Both cases predict the same fiber directions along the main mold perpendicular axis and the same 2D fabric flat pattern (Fig. 19).

2. With the geometrical simulation, large fabric deformations occur (up to 80°) for the D1 draping; however, smaller fabric deformations occur (up to 60°) for the D2 draping (Fig. 18).

3. For the inner areas on the two domes, the geometrical draping method predicts smaller nonwoven fabric shear angles for the two case draping D1 and D2 (marked with E, F, G, and H) (see Fig. 18).

4. For the outer areas, both cases predict different fiber orientations in regions A, B, and C (see Fig. 18). The main differences occur in the concave area between the two hemispheres (region B) and outer areas of the large hemisphere (region A) and small hemisphere (region C). With the geometrical simulation, on both, the larger and the smaller hemispheres, large fabric deformations occur (up to 70°).

This difference can be explained from the D1 draping, which starts from the top of the small hemisphere and extends outward from the highest point at the edge, resulting in gradually downward moving fibers and fiber disentanglement. When the fiber reaches the edge of the intersection fillet (position C), it will extend from that position onward (marked A), up and over the top of the larger hemisphere, resulting in a large fabric deformation at the outer area of the hemispheres and fiber interlacing.

The D2 draping starts from the top of the large hemisphere and extends outward from the lower point at the edge, resulting in gradually downward moving fiber and fiber disentan-

http://dx.doi.org/10.5772/61667

outer areas of the large hemisphere (region A) and small hemisphere (region C). With the geometrical simulation, on both, the larger and the smaller hemispheres, large fabric deformations occur (up to 70°).

This difference can be explained from the D1 draping, which starts from the top of the small hemisphere and extends outward from the highest point at the edge, resulting in gradually downward moving fibers and fiber disentanglement. When the fiber reaches the edge of the intersection fillet (position C), it will extend from that position onward (marked A), up and over the top of the larger hemisphere, resulting in a large fabric deformation at the outer area of the hemispheres and fiber interlacing.

The D2 draping starts from the top of the large hemisphere and extends outward from the lower point at the edge, resulting in gradually downward moving fiber and fiber disentanglement. When the fiber reaches the edge of the intersection fillet, it will extend from that position onward (marked B), up and over the top of the larger hemisphere, resulting in a large fabric deformation at the outer area of the hemispheres and fiber interlacing.

glement. When the fiber reaches the edge of the intersection fillet, it will extend from that position onward (marked B), up and over the top of the larger hemisphere, resulting in a large fabric deformation at the outer area of the hemispheres and fiber interlacing.

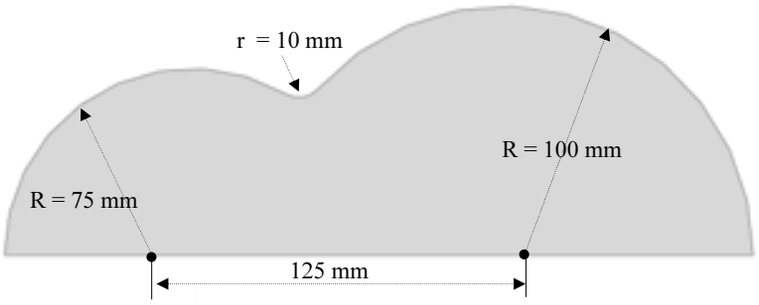

Figure 14. *Schematic view of the double dome*

Figure 14. Schematic view of the double dome

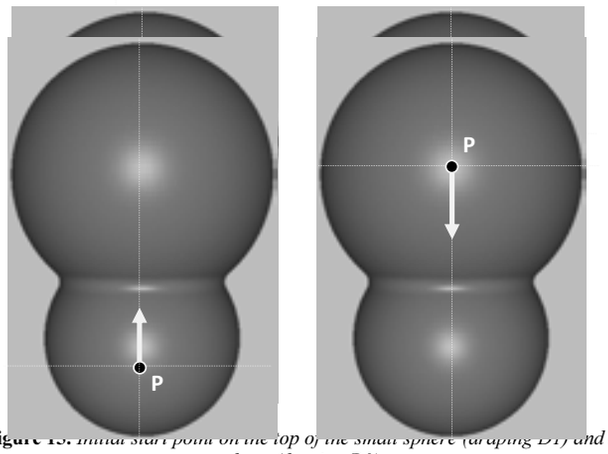

12

Figure 15. *Initial start point on the top of the small sphere (draping D1) and on the large sphere (draping D2)*

Figure 15. Initial start point on the top of the small sphere (draping D1) and on the large sphere (draping D2)

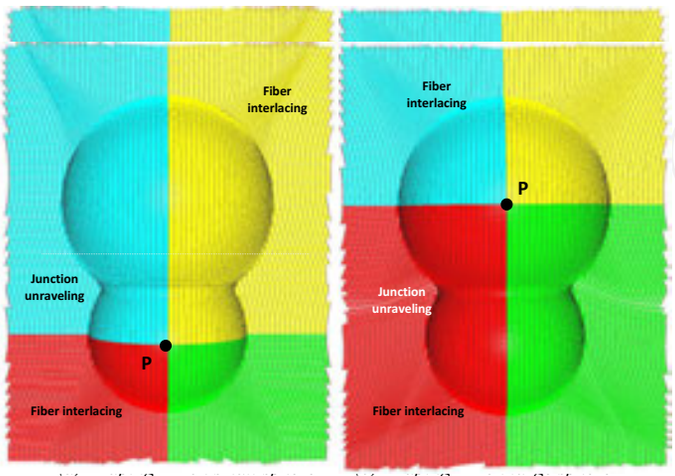

(a) Draping D1 on small sphere (b) Draping D2 on large sphere

Figure16. *3D draping results of nonwoven fabric on double dome*

Figure 16. 3D draping results of nonwoven fabric on double dome

13

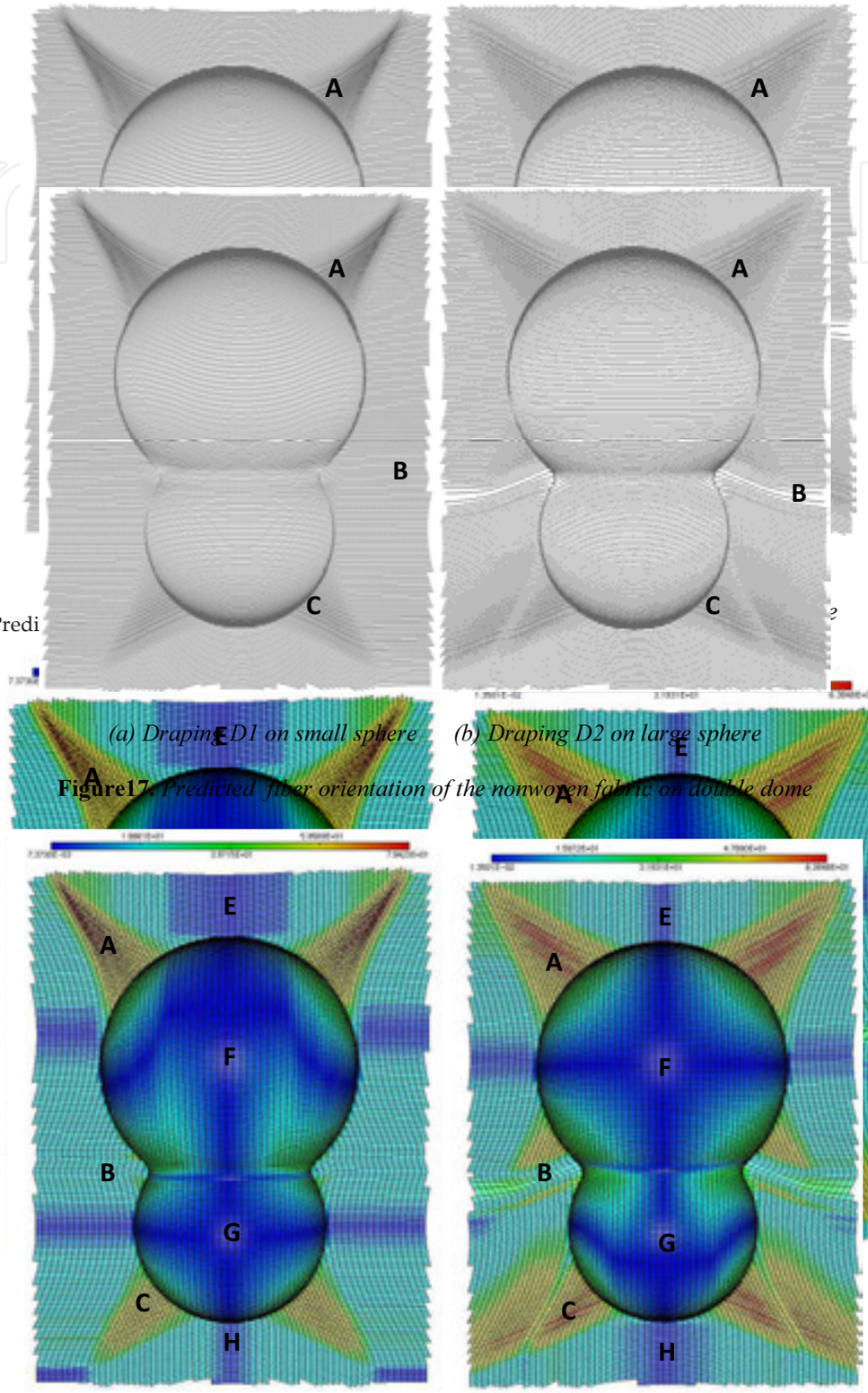

Figure 17. Predi

(a) Draping D1 on small sphere (b) Draping D2 on large sphere

Figure17. *Predicted fiber orientation of the nonwoven fabric on double dome*

Figure 18. *Shear angle of draped nonwoven fabric of drape D1 and drape D2*

Figure 18. Shear angle of draped nonwoven fabric of drape D1 and drape D2

14

http://dx.doi.org/10.5772/61667

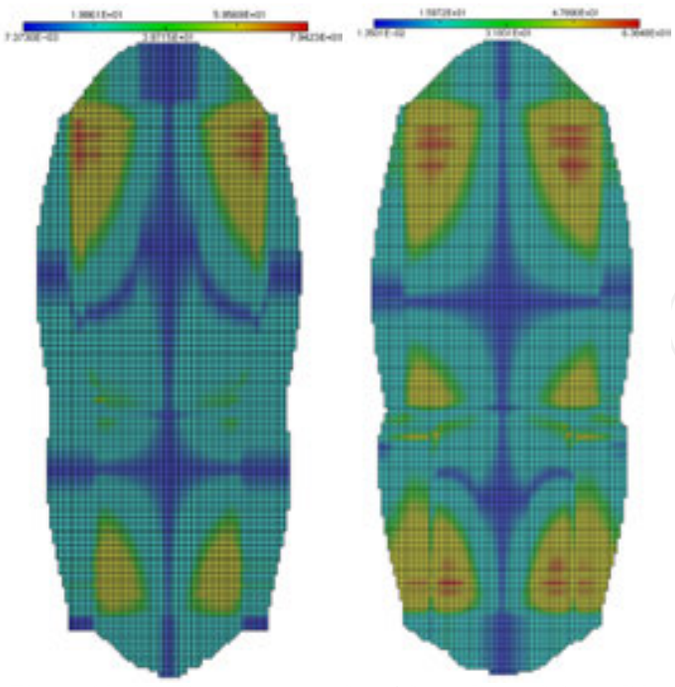

Figure 19. *2D Flat pattern results of drape D1 and drape D2*

Figure 19. 2D Flat pattern results of drape D1 and drape D2

4. Conclusions

This paper presented several aspects of the draping of nonwoven fabric composite on complex mold geometry. The kinematic approach is well-adapted to preliminary design level. It is based on a modified MOSAIC algorithm, which is suitable to generate a regular quad mesh representing the draping of woven fabric on curved surfaces. In order to obtain suitable deformation of nonwoven during the draping operation, modified kinematic algorithm based on the shear angle criterion is proposed. This algorithm allowed step-by-step stretching of weaving yarns using iterative procedure. Some numerical examples concerning the draping of woven or nonwoven fabric are presented in order to demonstrate the efficiency of the proposed approach. They provide a good correlation with the experimental results.

Author details

Abel Cherouat* and Houman Borouchaki*

15

*Address all correspondence to: abel.cherouat@utt.fr; houman.borouchaki@utt.fr

University of Technology of Troyes, Charles Delaunay Institute/GAMMA-INRIA Project Team, Troyes, France

References

[1] Bannister M. (2001), "Challenges for composites into the next millennium – a reinforcement perspective". *Composites Part A*, 32:901-10.

[2] Laurenzi S., Casini A., Pocci D. (2014), "Design and fabrication of a helicopter unitized structure using resin transfer moulding", *Composites Part A: Appl Sci Manufact*, 67: 221-232.

[3] Prodromou A.G, Chen J. (1997) "On the relationship between shear angle and wrinkling of textile composite preforms", *Composites Part A*, 28A, 491-503.

[4] Hou M., Ye L., Mai Y.W. (1997), "Manufacturing process and mechanical properties of thermoplastic composite components". *J Mater Process Technol*, 63: 334-338.

[5] Campbell F.C. (2004), *Manufacturing Processes for Advanced Composites*, Elsevier Advanced Technology, Oxford.

[6] Trochu F., Ruiz E., Achim V., Soukane S. (2006), "Advanced numerical simulation of liquid composite molding for process analysis and optimization", *Composites Part A: Appl Sci Manufact*, 37: 890-902.

[7] Ivanov D.S., Ivanov S.V. (2015), "Modelling the structure behaviour of 2D and 3D woven composites used in aerospace applications", *Polym Compos Aerospace Indus*, 21-52.

[8] Mark C., Taylor H.M. (1956), "The fitting of woven cloth to surfaces", *J Text Inst*, 47: 477-488.

[9] Breen D., House D., Wozny M. (1994), "A particle–based model for simulating the draping behavior of woven cloth". *Text Res J* 64, 11 663-685.

[10] Trochu F., Hammami A., Benoit Y. (1996), Prediction of fibre orientation and net shape definition of complex composite parts. *Composites Part A*, 27:319-328.

[11] Vandeurzen P., Ivens J., Verpoest I. (1996), "A three dimensional micro mechanical analysis of woven fabric composites: I. elastic analysis". *Compos Sci Technol*, 56:1317-1327.

[12] Ben Boubaker B., Haussy B., Ganghoffer J.F. (2007), "Discrete woven structure model: yarn-on-yarn friction", *Comptes Rendus Mécanique*, 335(3):150-158.

[13] Cordier F., Magnenat-Thalmann, N. (2002), "Real–time animation of dressed virtual humans". *Eurographics*, 21, 3.

[14] Van Der Ween F. (1991), "Algorithms for draping fabrics on doubly curved surfaces", *Int J Numer Methods Eng*, 31:1414-1426.

[15] Long A.C., Rudd C.D. (1994), "A simulation of reinforcement deformation during the production of preform for liquid moulding processes", *Proc Inst Mech Eng Part B J Eng Manuf*, 208: 269-278.

[16] Hancock S.G., Potter K.D. (2005), "Inverse drape modelling—an investigation of the set of shapes that can be formed from continuous aligned woven fibre reinforcements", *Composites Part A: Appl Sci Manufact*, 36(7): 947-953.

[17] Yin H., Peng X., Du T., Guo Z. (2014), "Draping of plain woven carbon fabrics over a double-curvature mold", *Composites Sci Technol*, 92(24): 64-69.

[18] Ivanov I., Tabiei A. (2002), "Flexible woven fabric micromechanical material model with fiber reorientation", *Mech Adv Mater Struct*, 9: 37-51.

[19] Kang T., Yu W. (1995), "Drape simulation of woven fabric by using the finite–element method", *J Text Instit*, 86(4): 635-648.

[20] Kato S., Yoshino T., Minami H. (1999), "Formulation of constitutive equations for fabric membranes based on the concept of fabric lattice model", *Engin Struct,* 21: 691-708.

[21] Boisse P., Cherouat A., Gelin J.C., Sabhi H. (1995), "Experimental study and finite element simulation of a glass fiber fabric shaping process", *Polym Compos,* 16(1): 83-95.

[22] Duhovic M., Mitschang P., Bhattacharyya D. (2011), "Modelling approach for the prediction of stitch influence during woven fabric draping", *Composites Part A*: *Appl Sci Manufact*, 42: 968-978

[23] Asthana R., Kumar A., Dahotre N.B. (2006), "Composites get in deep with new-generation engine", *Reinforced Plastics*, 50(11): 26-29.

[24] Prodromou A.G, Stepan V. Lomov, Ignaas Verpoest (2011), "The method of cells and the mechanical properties of textile composites", *Compos Struct*, 93(4): 1290-1299.

[25] Gatouillat G., Bareggi, Vidal-Sallé E., Boisse P. (2013), "Meso, modelling for composite preform shaping – Simulation of the loss of cohesion of the woven fibre network", *Composites Part A: Appl Sci Manufact*, 54: 135-144.

[26] Gereke T., Döbrich O., Matthias Hübner, Chokri Cherif (2013), "Experimental and computational composite textile reinforcement forming": *Composites Part A: Appl Sci Manufact*, 46: 1-10.

[27] Rozant O., Bourban PE., Manson JAE. (2000), "Drapability of dry textile fabrics for stampable thermoplastic preforms". *Composites: Part A,* 31: 1167-1177.

[28] Cherouat A., Borouchaki H., Giraud-Moreau L. (2011), "Mechanical and geometrical approaches applied to composite fabric forming", *Int J Mater Form*, DOI 10.1007/s12289-010-0692-5.

[29] Teik-Cheng Lim, Ramakrishna S. (2002), "Modelling of composite sheet forming: a review", *Composites Part A: Appl Sci Manufact*, 33: 515-537

[30] Warby M.K., Whiteman J.R., Jiang W.-G., Warwick P., Wright T. (2003), "Finite element simulation of thermoforming processes for polymer sheets", *Math Compu Simul*, 61: 209-218.

[31] Cherouat A., Borouchaki H., Billoët J.L. (2005), "Geometrical and mechanical draping of composite fabric", *Eur J Comput Mech*, 14 (6–7), 693-708.

[32] ElHami A., Radi B., Cherouat A. (2009), "Treatment of the composite fabric's shaping using a Lagrangian formulation", *Math Compu Model*, 49(7-8):1337-1349.

[33] Taha I., Abdin Y., Ebeid S. (2012), "Prediction of draping behavior of woven fabrics over double-curvature moulds using finite element techniques", *Int J Mater Mech Engin*, 1: 25-31.

[34] Vanclooster K., Lomov S.V., Verpoest I. (2009), "Experimental validation of forming simulations of fabric reinforced polymers using an unsymmetrical mould configuration", *Composites Part A: Appl Sci Manufact*, 40(4): 530-539.

[35] Potluri P., Sharma S., Ramgulam R. (2001), "Comprehensive drape modelling for moulding 3D textile preforms", *Composites Part A: Appl Sci Manufact*, 32(10): 1415-1424.

[36] Xue P., Peng X., Cao J. (2003), "A non-orthogonal constitutive model for characterizing woven composites", *Composites Part A*: 34: 183-193.

[37] Sharma S.B., Sutcliffe M.P.F. (2004), "A simplified finite element model for draping of woven material", *Composites Part A*, 35: 637-643.

[38] Fan J.P., Tang C.Y., Tsui C.P., Chan L.C. and Lee T.C. (2006), "3D finite element simulation of deep drawing with damage development", *Int J Mach Tools Manufact*, 46(9): 1035-1044.

[39] Heisley F., Haller, K. (1988) "Fitting woven fabric to surfaces in three dimensions". *J Text Instit 2*, 250-263.

[40] Weëen, F. (1991), "Algorithms for draping fabric on doubly–curved surfaces". *Int J Numer Meth Engin*, 31: 1415-1426.

[41] Robertson R., Hsiue E., Yeh G. (1984), "Fibre rearrangements during the moulding of continuous fibre composites", *Polym Composites*, 5: 191-197.

[42] Cherouat A., Billoët J.L. (2001), "Mechanical and numerical modelling of composite manufacturing processes deep-drawing and laying-up of thin pre-impregnated woven fabrics", *J Mat Proc. Technol*, 118: 460-471.

[43] Cherouat A., Borouchaki H. (2009), "Present state of the art of composite fabric forming: geometrical and mechanical approaches", *Mater* 2(4):1835-1857.

[44] Vanclooster K., Lomov S.V., Verpoest I. (2009), "Experimental validation of forming simulations of fabric reinforced polymers using an unsymmetrical mould configuration", *Composites Part A: Applied Science and Manufacturing* 40 (4): 530-539.

[45] De Luca, P., Lefébure, P., Pickett, A. (1998), "Numerical and experimental investigation of some press forming parameters of two fibre reinforced thermoplastics: APC2–AS4 and PEI–CETEX", *Composites Part A,* 29: 101-110.

IntechOpen

IntechOpen

IntechOpen

IntechOpen